REGULAR ARTICLE

Electrochemical aspects of restricted rhenium(I)-based supramolecular complexes with semi-rigid benzimidazolyl and rigid hydroxyquinone ligands

SARITA YADAV[a], MOOKAN NATARAJAN[a], MALAICHAMY SATHIYENDIRAN[b],* and SANDEEP KAUR-GHUMAAN[a],* ⓘ

[a] Department of Chemistry, University of Delhi, Delhi 110 007, India
[b] School of Chemistry, University of Hyderabad, Hyderabad, Telangana 500 046, India
E-mail: msathi@uohyd.ac.in; skaur@chemistry.du.ac.in

Abstract. Supramolecular coordination complex $[(Re(CO)_3)_2(dhnq)(L^2)]$ (**3**) containing two *fac*-$Re(CO)_3$ cores, rigid dianionic dhnq (H_2-dhnq = 6,11-dihydroxy-5,12-naphthacenedione) motif and semi-rigid ditopic nitrogen donor 1,2-bis(2-nonylbenzimidazol-1-ylmethyl)benzene (*o*-Nbenzbix = L^2) was synthesized. Compounds *o*-Nbenzbix and **3** were characterized using various analytical and spectroscopic methods. The electrochemical properties of **3** were studied using cyclic voltammetric measurements. SCCs $[(Re(CO)_3)_2(dhnq)(L^1)]$ (**1**) and $[(Re(CO)_3)_2(dhaq)(L^1)]$ (**2**) possessing *p*-xylene spacer 1,4-bis(2-nonylbenzimidazol-1-ylmethyl)benzene (L^1) and 1,4-dihydroxy-9,10-anthraquinone (H_2-dhaq) were also synthesized as reported previously. SCCs **1**–**3** were investigated *via* electrochemical methods. A plot of the Randles-Sevcik equation yielded a straight line for complex **3** thus, establishing that the redox processes were diffusion-controlled.

Keywords. Rhenium; nonylbenzimidazole; hydroxyquinone; supramolecular coordination complex; electrochemistry.

1. Introduction

Inspired by the involvement of various supramolecular complexes in the natural processes researchers have developed functional supramolecular coordination complexes (SCCs) with varying shapes and geometries in the past few decades.[1,2] Moreover, due to the exciting structures and properties, SCCs have potential applications in different fields including host-guest chemistry (molecular sensors), sieving, probes for environmental changes, molecular flasks, electron storage, membrane transport agents, light emission, anti-cancer agents and catalysis. Scientists are also making efforts to use metallacycles as functional devices at molecular levels.[3–12] The supramolecular systems can be easily functionalized with photo- and redox-active units, making their redox properties of great interest to the scientists. The discrete, stable redox-active SCCs have been studied for their electrochemical properties including site-specific multiple electron reductions, reversible reduction/oxidation and inter-valence charge transfer to find out their electron uptake ability as well as the electron-transfer potential in the supramolecular aggregates. Moreover, redox-based photochemistry of electro-active materials is fast gaining attention in display devices, fibre-optics, electrochemical sensing, information storage and artificial photosynthesis, photovoltaics, NIR absorption/emission, communication and medical fields.[13,14]

SCCs with a $Re(CO)_3$ core are unique due to their stability and robustness.[15,16] The Re-based rectangular assemblies with electrochemically-active ligands are potential redox-stable materials that can be charged reversibly. The $[fac$-$Re(CO)_3$(diimine)] unit(s) containing SCCs and acyclic complexes are powerful electron acceptors and display good redox stability.[17–25] The electrochemistry of acyclic complexes

containing *fac*-Re(CO)$_3$ unit are prevalent in the literature. However, the electrochemical studies of *fac*-Re(CO)$_3$-core based SCCs containing quinone unit(s) are very limited.[26–29] The electrochemical properties of SCCs are determined by the arrangement of spacer units of ligands which tune the communication between the ligands in the SCCs.[30,31] While, the degree of metal-metal interaction present in the complex affect the oxidation processes.[27,28,32]

The cyclic coordination of non-innocent ligands with rhenium ions should result in redox-stable self-assembled SCCs. In this regard, synthesis and structural characterization of dinuclear SCCs [(Re(CO)$_3$)$_2$(dhnq)(L^1)] (**1**) and [(Re(CO)$_3$)$_2$(-dhaq)(L^1)] (**2**) (where L^1 = *p*-Nbenzbix, 1,4-bis(2-nonylbenzimidazol-1-ylmethyl)benzene; dhnq = 1,4-dihydroxy-9,10-anthraquinone and dhaq = 6,11-dihydroxy-5,12-naphthacenedione) were reported recently (Figure 1).[33] The complexes **1** and **2** possess redox active (non-innocent) anthraquinone units, two *fac*-Re(CO)$_3$ cores, and benzimidazolyl units. As a continuation of the work, herein, we report a new ligand 1,2-bis(2-nonylbenzimidazol-1-ylmethyl)benzene (*o*-Nbenzbix = L^2) (Figure 1), and its complex [(Re(CO)$_3$)$_2$(dhnq)(L^2)] (**3**). The two benzimidazolyl units in *o*-Nbenzbix after coordinating with metal cores may lie parallel to each other with the distance of π···π contact. The use of *o*-Nbenzbix would result in redox active SCCs *via* communication between the ligand cores.[34] The ligand and complex **3** were characterized using various analytical and spectroscopic methods. The electrochemical properties of **1–3** were studied and compared.

2.   Experimental

2.1   *Apparatus and material*

All starting materials and products were found to be air and moisture stable and no specific precautions were taken to exclude air while using solvothermal methods. Starting materials such as Re$_2$(CO)$_{10}$, H$_2$-dhnq, H$_2$-dhaq, 2-nonyl-benzimidazole, 1,4-bis(bromomethyl)benzene, 1,2-bis(bromomethyl)benzene, and KOH were procured from commercial sources and used as received. Complexes **1** and **2** were synthesized using reported methods.[33] Aromatic solvents were purified by conventional procedures and were distilled prior to use. Conventional synthetic methods were routinely carried out in room atmosphere. Elemental analysis was performed on a Elementar Analysen systeme GmbH Vario EL-III instrument. FTIR spectra were recorded on a Perkin-Elmer FTIR-2000 spectrometer. ^{1}H-NMR spectra were recorded on Bruker AMX-400 FT-NMR and

Jeol JNMECX-400P spectrometers. Electrochemical measurements were conducted in acetonitrile and dichloromethane with 0.1 M tetrabutylammoniumhexafluorophosphate (Sigma-Aldrich, electrochemical grade) as supporting electrolyte that was dried in vacuum at 383 K. Cyclic voltammetry was carried out using an Autolab potentiostat with a GPES electrochemical interface. The working electrode was a glassy carbon disc (diameter 3 mm, freshly polished) for cyclic voltammetry. Platinum was used as the counter electrode. The reference electrode was a non-aqueous Ag/Ag$^+$ electrode (0.010 M AgNO$_3$ in acetonitrile). All the potentials are quoted against the ferrocene-ferrocenium couple (Fc/Fc$^+$); ferrocene was added as an internal standard at the end of the experiments. All solutions were prepared from dry acetonitrile and dichloromethane (Sigma-Aldrich, spectroscopic grade, dried with molecular sieves, MS 3 Å).

2.2   *Synthesis of o-Nbenzbix (L^2) ligand*

Ligand *o*-Nbenzbix was synthesized by following the reported procedure in which a mixture of powdered KOH and 2-nonylbenzimidazole in THF was placed in a round-bottom flask. The resulting suspension was stirred for 2 h. A solution of *o*-xylylenedibromide in THF was slowly added to the yellowish solution. The final reaction mixture was then stirred continuously overnight. The solvent was removed under reduced pressure and the residue was poured into water. The compound was extracted with dichloromethane three times. The combined organic extracts were washed with water, dried over Na$_2$CO$_3$ to remove traces of water, and concentrated. The crude product was obtained as yellow colored powder. Yield: ∼ 75%; Anal. Calcd for C$_{40}$H$_{54}$N$_4$ (M$_r$ 590.43): C, 81.31; H, 9.21; N, 9.48; Found: C, 80.98; H, 9.33; N, 9.69; ^{1}H NMR (400 MHz, 298 K, ppm in DMSO-d_6): 7.82 (d, 2H), 7.3 (t, 2H), 7.22 (t, 2H), 7.19 (m, 2H), 7.05 (d, 2H), 6.67 (m, 2H), 5.3 (s, 4H, methylene), 2.75 (t, 4H), 1.8 (m, 8H), 1.25 (m, 20H), 0.87 (t, 6H).

2.3   *Synthesis of complex [(Re(CO)$_3$)$_2$(dhnq)(L^2)] 3*

A mixture of Re$_2$(CO)$_{10}$ (0.4 mmol), *o*-Nbenzbix (0.4 mmol) and H$_2$-dhnq (0.4 mmol) in toluene (10 mL) in a Teflon flask was placed in a steel bomb. The bomb was placed in an oven maintained at 160 °C for 48 h and then cooled to 25 °C. Dark green-colored powder of **3** was obtained which was separated by filtration and washed with toluene. Yield: ∼56% (0.04 g); Anal. Calcd for C$_{64}$H$_{62}$N$_4$O$_{10}$Re$_2$ (M$_r$ 1419.63): C, 54.15; H, 4.40; N, 3.95; Found: C, 52.25; H, 4.21; N, 3.58; IR (CH$_3$COCH$_3$, cm^{-1}): ν$_{C=O}$ 2008, 1900, 1878 cm^{-1}; ^{1}H NMR (400 MHz, 298 K, ppm in DMSO-d_6): 6.2–8.5 (dhnq, Nbenzbix), 5.3–5.7 (methylene, Nbenzbix), 2.5 (nonyl), 1.24 (nonyl), 0.85 (nonyl).
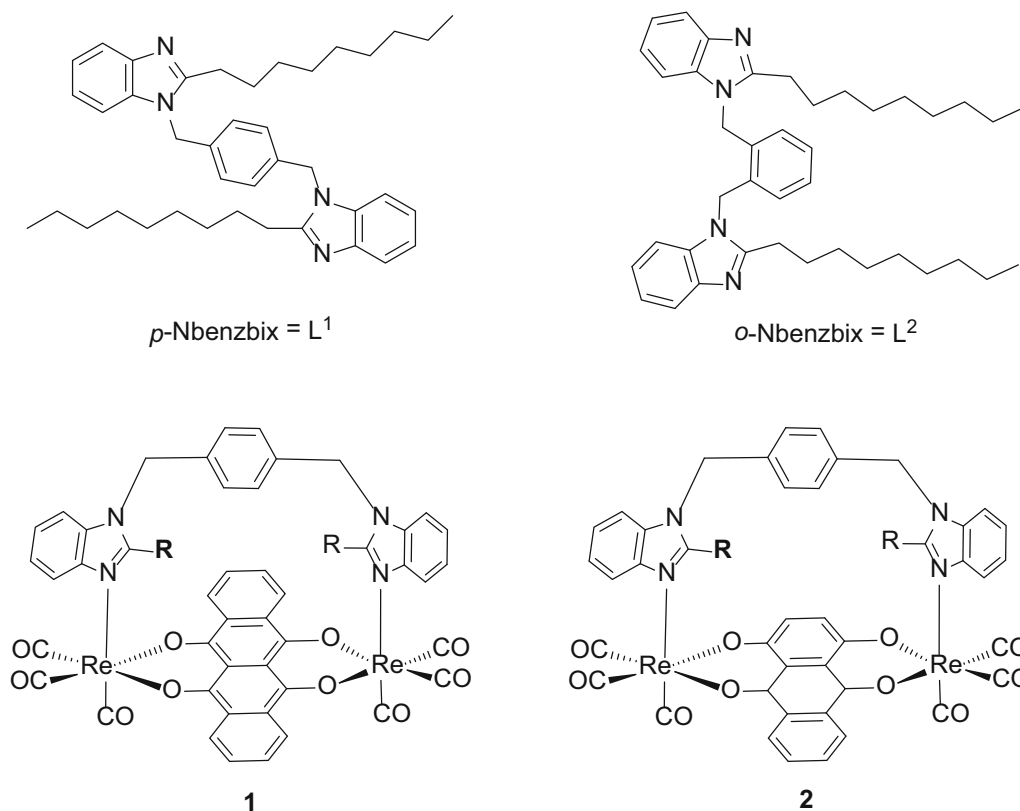
Figure 1. Structures of ligands (L^1 and L^2)and SCCs **1**, and **2** (R = –(CH$_2$)$_8$CH$_3$).

3. Results and Discussion

3.1 *Synthesis and characterization*

Ligand L^1 and complexes **1** and **2** were synthesized as reported in the literature.[33] X-ray crystal structure for complex **1** was reported earlier.[33] Ligand L^2 was synthesized from the reaction of 1,2-bis(bromomethyl)benzene and 2-nonylbenzimidazole in presence of KOH in THF (Scheme 1).

Complex **3** was prepared following a similar procedure using *o*-Nbenzbix, Re$_2$(CO)$_{10}$ and H$_2$-dhnq in toluene (Scheme 2).[32]

The ^{1}H NMR spectrum of *o*-Nbenzbix shows two doublets and two triplets at 7.82, 7.05, 7.3 and 7.22 ppm corresponding to the benzimidazolyl unit and two multiplets at 7.19 and 6.67 ppm for *o*-phenylene protons (Figure S1, Supplementary Information). The five chemical resonances in the aliphatic region correspond to the nonyl group of the ligand. The disappearance of the NH proton peak at 13 ppm, and the appearance of a singlet at 5.3 (methylene) ppm, indicates the formation of ligand L^2. The proton ratio of 2-nonylbenzimidazolyl unit and *o*-phenylene unit is 2:1, confirming the stoichiometry of the ligand. Compared to free 1,2-bis(bromomethyl)benzene, the chemical shifts of protons of methylene and *o*-phenylene unit in L^2 are shifted in the downfield region. The possibility of existence of isomeric forms of L^2 in the solution and their interconversion into each other in the ^{1}H NMR timescale is not omitted.

The FTIR spectrum of complex **3** display three carbonyl stretching frequencies at 2008, 1900 and 1878 cm^{-1}, which correspond to the *fac*-Re(CO)$_3$ core in the complex similar to the values reported for complexes **1** (2008, 1903, 1875 cm^{-1}) and **2** (2009, 1899, 1881 cm^{-1}).[33] The ^{1}H NMR spectrum of complex **3** displayed chemical resonances with complicated patterns (Figure S2, Supplementary Information). However, the ratio of methylene proton: aromatic protons (*o*-Nbenzbix and dhnq) is 4:20, confirming the formation of SCC. In addition, a significant shift in the chemical resonance values for the aromatic protons was also observed. The chemical shift values for the methylene protons in complex **3** shifted downfield compared to those in the free *o*-Nbenzbix ligand.

The mass spectrum of complex **3** displays molecular ion peak m/z 1421.3553 for M$^+$ (Figure S3, Supplementary Information). The theoretical value for these molecular ion peaks with isotopic distribution peaks
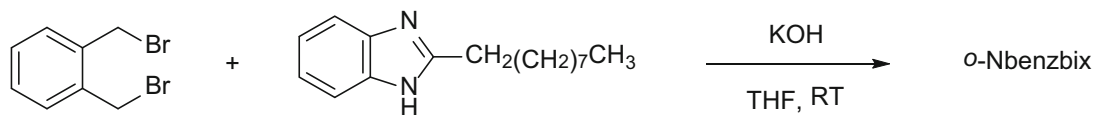
Scheme 1. Synthesis of *o*-Nbenzbix L².
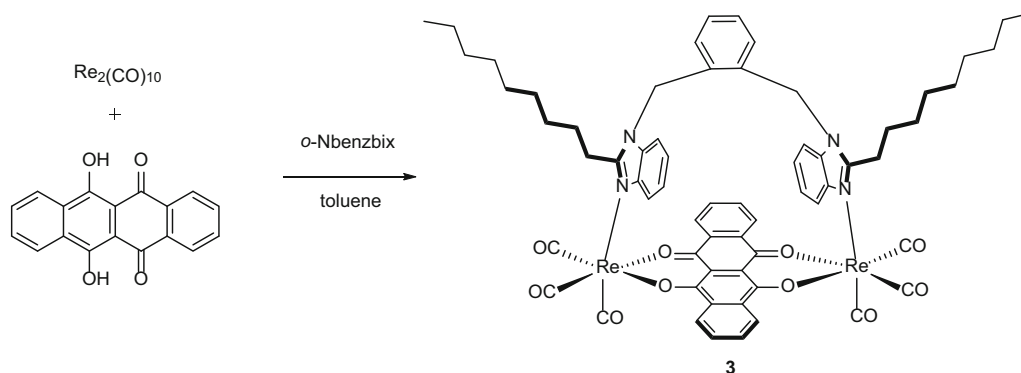
Scheme 2. Synthesis of SCC **3**.

matched well with the obtained peaks (Figure S4, Supplementary Information). The ESI-MS and elemental analysis confirm the formation of the complex **3** in high purity.

3.2 *Electrochemical investigations*

Electrochemical properties of the dinuclear complexes are dependent on the nature of the bridging ligands, relevant cyclic voltammograms (CVs) are shown in Figure 2. The presence of redox-active quinone ligands in the complexes is expected to make them redox-active and hence, exhibit rich electrochemistry. The cyclic voltammograms of the complexes **1**, **2** and **3** in dichloromethane displayed two one-electron reduction waves with E_{pc} values for the three complexes as follows: **1** (-1.57 and -2.06 V), **2** (-1.33, -1.85) and **3** (-1.51, -2.00 V) (Table 1). The reduction waves can be assigned as $[X]^{2-} \rightarrow [X]^{3\bullet-}$ and $[X]^{3\bullet-} \rightarrow [X]^{2-}$ (X = dhnq or dhaq).[35,36] The first and second quinone reductions for the assemblies (**1–3**) were cathodically shifted compared to the redox potentials of the free dianionic quinone analogs.[37] The large differences in potentials between the two successive reduction processes are due to the large thermodynamic stability for the intermediate radical anions, $\mathbf{1^{\bullet-}}$, $\mathbf{2^{\bullet-}}$ and $\mathbf{3^{\bullet-}}$. The clip ligands (L¹ or L²) contribute no redox properties within the solvent window, as evidenced by a CV investigation. The first reduction in all three complexes was reversible while the second reductions were irreversible. Similar
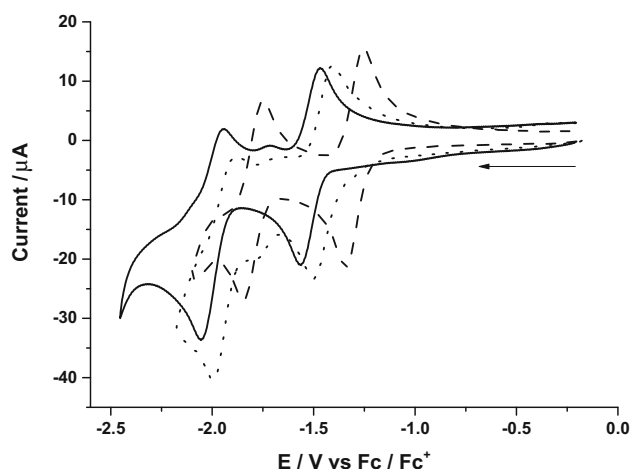

Figure 2. CVs for 1 mM of complexes **1** (solid line), **2** (dashed line) and **3** (dotted line) in dichloromethane at a scan rate of 0.1 V/s.

behavior was observed for the CVs in acetonitrile (Table 1). Apparently, because of the large metal-metal separation, oxidation and reduction of the two metal centers occur simultaneously, *i.e.,* the metals behave in an essentially independent manner. The fact that the bridged rings are not involved in the conjugation may also be an important factor. In the case of potential difference, the complex **2** reduced at lower potential than **1** and **3** (Figure 2).

This is probably due to the absence of one arene ring less in naphthacenedione in complex **2** than in anthraquinone ligand in complexes **1** and **3**. Moreover, the Re(I/0) reduction was not observed within the

Table 1. Electrochemical data for SCCs **1–3** in dichloromethane and acetonitrile.

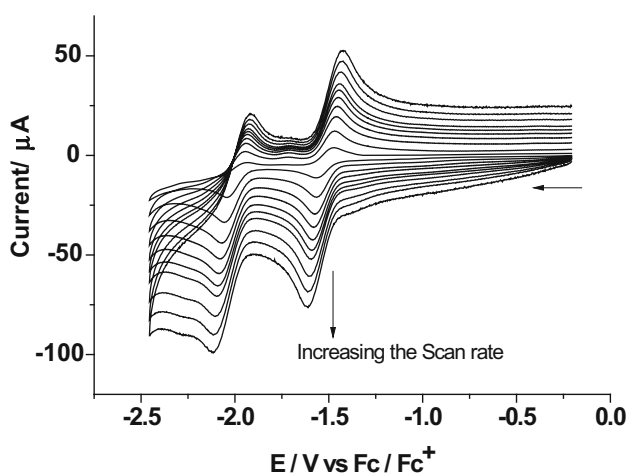| | Dichloromethane | | | | | Acetonitrile | | | |
| | Reduction | | | | Oxidation | Reduction | | | Oxidation |
Complex	E_{pc}/V	E_{pa}/V	$E_{1/2}$/V	i_{pa}/i_{pc}	E_{pa}/V	E_{pc}/V	E_{pa}/V	$E_{1/2}$/V	E_{pa}/V
1	−1.57	−1.47	−1.52	0.582	0.58	−1.47	−1.39	−1.43	0.90
	−2.06	–	–	0.053	1.01	−1.93	–		1.27
					1.44				–
2	−1.33	−1.25	−1.29	0.734	0.64	−1.27	−1.20	−1.23	0.75
	−1.85	–	–	0.249	1.04	−1.79	–	–	1.11
	−2.01				1.35				1.43
3	−1.51	−1.41	−1.46	0.542	0.53	−1.46	−1.41	−1.43	0.63
	−2.00	–	–	0.071	0.97	−1.95	–	–	1.24
	−2.13				1.36				–

Figure 3. CVs for complex **1** (1 mM) in CH$_2$Cl$_2$ at different scan rates (0.025, 0.1, 0.2, 0.3, 0.4, 0.5, 0.6, 0.8, 1.0 and 1.2 V/s).
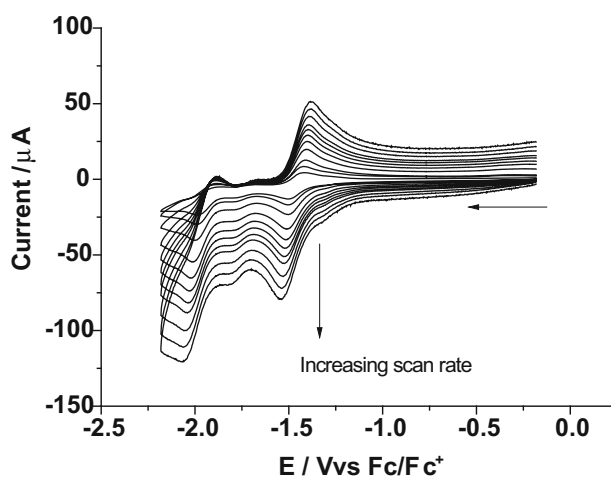

Figure 5. CVs for complex **3** (1 mM) in CH$_2$Cl$_2$ at different scan rates (0.025, 0.05, 0.1, 0.2, 0.3, 0.4, 0.5, 0.6, 0.8, 1.0 and 1.2 V/s).
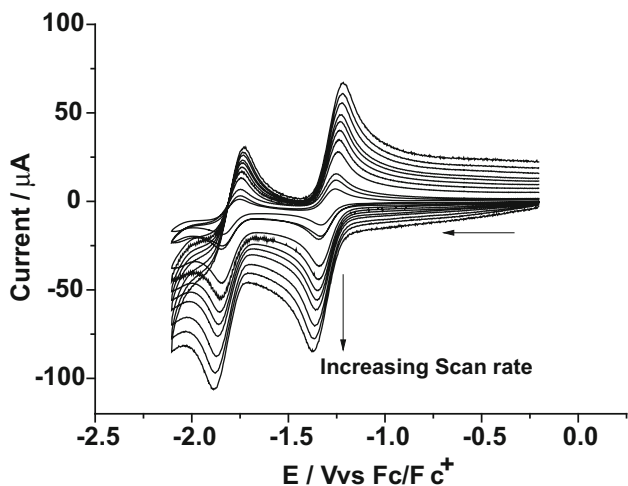

Figure 4. CVs for complex **2** (1 mM) in CH$_2$Cl$_2$ at different scan rates (0.025, 0.05, 0.1, 0.2, 0.3, 0.4, 0.5, 0.6, 0.8, 1.0 and 1.2 V/s).

Table 2. Diffusion current for complexes **1–3** in dichloromethane and acetonitrile.
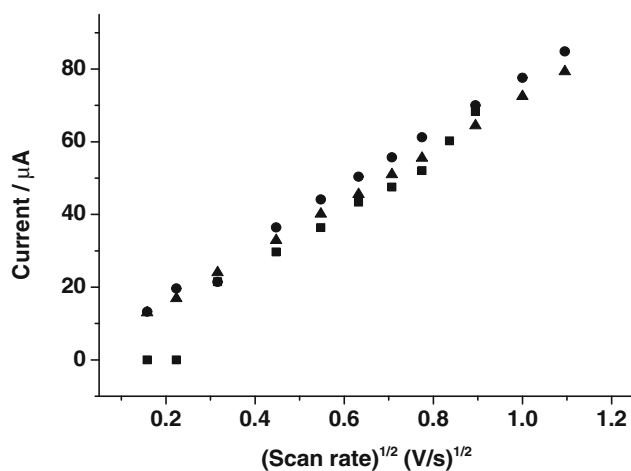
| | Diffusion current cm^2/s | | | |
| | Dichloromethane | | Acetonitrile | |
Complex	E_{pc}^1	E_{pc}^2	E_{pc}^1	E_{pc}^2
1	0.1545	0.1693	0.0155	0.0151
2	0.1165	0.1771	4.6306	0.0828
3	0.9797	0.2133	0.0011	0.1545

solvent window (+0.5 to −2.9 V). In addition, the three complexes also displayed irreversible oxidation processes (Table 1).

One of the reasons for this irreversibility could be probably due to the intolerance of the Re(I) center to change its oxidation state without undergoing drastic changes in its coordination sphere. Further, on varying

Table 3. Slope (i_p) of complexes **1–3** in dichloromethane and acetonitrile.

Complex	Dichloromethane		Acetonitrile	
	E_{pc}^1/V	E_{pc}^2/V	E_{pc}^1/V	E_{pc}^2/V
1	88.826	92.996	23.187	27.801
2	77.114	95.105	486.263	65.050
3	70.737	104.383	73.297	88.838

Figure 7. Randles-Sevcik relation plot of **1** (filled square), **2** (filled circle) and **3** (filled triangle) with peak currents (for E_{pc}^2, second reduction) for varying currents *vs* the square root of scan rate (negative sign for current is ignored).

$$D^{1/2} = i_p/(2.69 \times 10^5)\, n^{3/2} A\, C\, v^{1/2} \qquad (3)$$

Where, i_p is the peak current of reduction/oxidation process, n is the number of electrons per species, A is the area of electrode in contact with electrolytic solution, D is the diffusion coefficient, C is the electrolyte concentration, F is the Faraday constant, R is the Rydberg constant, T is the temperature and v is the scan rate. This equation clearly predicts that the reduction/oxidation peak position is proportional to the square root of scan rates and the redox processes are diffusion-controlled.

Figure 6. Randles-Sevcik relation plot of **1** (filled circle), **2** (filled triangle) and **3** (filled square) with peak currents (for E_{pc}^1, first reduction) for varying currents *vs.* the square root of scan rate (negative sign for current is ignored).
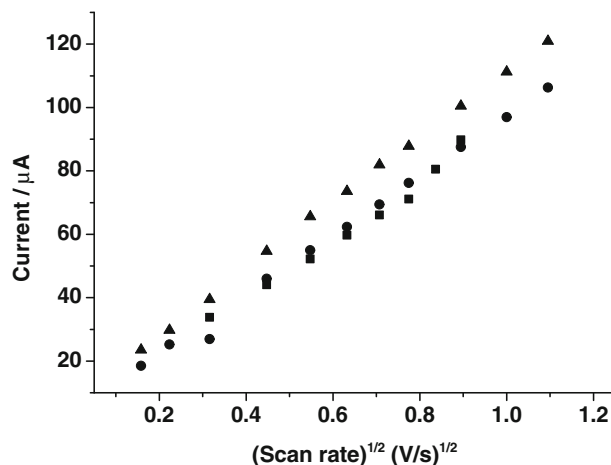
the scan rate from 0.025–1.2 V/s (in dichloromethane and acetonitrile), it has been observed that the peak currents for the first reduction are almost constant. However, the second reduction shifted towards reversibility from irreversible reduction with a very slow rate (Figures 3, 4 and 5, Tables 1, 2 and 3 and Figures S5–S8, Tables S1–S2, Supplementary Information).

It is a well-established fact that the reduction and oxidation processes in an electrochemical reaction are kinetic in nature. There is a systematic shift in the redox peak position with scan rate in cyclic voltammograms. A theoretical model has been developed by Randles and Sevcik to predict how peak current in the reduction/oxidation process depends on the scan rate (Figures 6 and 7).[38,39] The relation between these parameters is given by the following formulae that are known as Randles-Sevcik equations (1–3).

$$i_p = 0.4463\, n\, FAC \left\{ \frac{nFvD}{RT} \right\}^{1/2} \qquad (1)$$

(or)

$$i_p = (2.69 \times 10^5)\, n^{3/2} A\, C\, D^{1/2} v^{1/2} \qquad (2)$$

4. Conclusions

Re(I) based dinuclear, heteroleptic supramolecular coordination complex **1** was synthesized using newly designed semi-rigid ditopic benzimidazolyl ligand and hydroxyquinone. The electrochemical properties of **1–3** were studied using cyclic voltammetry. Electrochemical properties of SCCs **1–3** are dependent on the nature of the bridging ligands. The results reveal that the reduction processes for **1–3** are based on the quinone motif framework.[40–47]

Supplementary Information (SI)

The Supplementary Information includes NMR, ESI-MS and electrochemical data. Supplementary Information is available at www.ias.ac.in/chemsci.

Acknowledgements

References

1. Stang P J and Olenyuk B 1997 Molecular architectures: coordination as the motif in the rational design of supramolecular metallacyclic *Acc. Chem. Res.* **30** 502
2. Ruben M, Rojo J, Salguero F J R, Uppadine L H and Lehn J M 2004 Grid-type metal ion architectures: functional metallosupramolecular arrays *Angew. Chem. Int. Ed.* **43** 3644
3. Slone R V, Benkstein K D, Belanger S, Hupp J T, Guzei I A and Rheingold A L 1998 Luminescent transition-metal-containing cyclophanes ("molecular squares"): covalent self-assembly, host-guest studies and preliminary nanoporous material applications *Coord. Chem. Rev.* **171** 221
4. Sun S S and Lees A J 2002 Transition metal based supramolecular systems: synthesis, photophysics, photochemistry and their potential applications as luminescent anion chemosensors *Coord. Chem. Rev.* **230** 171
5. Thanasekaran V, Liao R T, Liu Y H, Rajendran T, Rajagopal S and Lu K L 2005 Metal containing molecular rectangles: synthesis and photophysical properties *Coord. Chem. Rev.* **249** 1085
6. Sun S S and Lees A J 2000 Self-assembly triangular and square Rhenium(I) tricarbonyl complexes: A comprehensive study of their preparation, electrochemistry, photophysics, photochemistry and host-guest properties *J. Am. Chem. Soc.* **122** 8956
7. Sathiyendiran M, Chang C H, Chuang C H, Luo T T, Wen Y S and Lu K L 2007 Rigidity-modulated conformation control: a strategy for incorporating flexible building motif into metallcycles *Dalton Trans.* **19** 1872
8. Sathiyendiran M, Wu J Y, Velayudham M, Lee G H, Peng S M and Lu K L 2009 Neutral metallacyclic rotors *Chem. Commun.* **25** 3795
9. Rajendran T, Manimaran B, Lee F Y, Chen P J, Lin S C, Lee G H, Peng S M, Chen Y J and Lu K L 2001 Self-assembly of tetrametallic square [Re$_4$(CO)$_{12}$Br$_4$(μ-pz)$_4$] (pz= pyrazine)from [Re(CO)$_4$Br(pz)]. A mechanistic approach *J. Chem. Soc. Dalton Trans.* **22** 3346
10. Manimaran B, Thanasekaran P, Rajendran T, Liao R T, Liu Y H, Lee G H, Peng S M, Rajagopal S and Lu K L 2003 Self-assembly of octarhenium-based neutral luminescent rectangular prisms *Inorg. Chem.* **42** 4795
11. Cook T R and Stang P J 2015 Recent developments in the preparation and chemistry of metallacycles and metallacages *via* coordinaton *Chem. Rev.* **115** 7001
12. Audebert P and Miomandre F 2013 Electrofluorochromism: from molecular systems to set-up and display *Chem. Sci.* **4** 575
13. Kaim W 2011 Concepts for metal complex chromophores absorbing in the near infrared *Coord. Chem. Rev.* **255** 2503
14. Hupp J T 2006 Rhenium-linked multiporphyrin assemblies: synthesis and properties. In: *Non-Covalent Multi-Porphyrin Assemblies. Structure and Bonding* E Alessio (Ed.) Vol. 121 (Springer: Berlin, Heidelberg) p. 145
15. Sathiyendiran M, Tsai C C, Thanasekaran P, Luo T T, Yang C I, Lee G H, Peng S M and Lu K L 2011 Organometallic calixarenes: Sycee like tetrarhenium(I) cavitands and tunable size, colour, functionality and coin-slot complexation *Chem. Eur. J.* **17** 9857
16. Gupta D, Rajakannu P, Shankar B, Hussain F and Sathiyendiran M 2014 Synthesis and crystal structure of a wheel-shaped supramolecular coordination complex *J. Chem. Sci.* **126** 1501
17. Louie M W, Liu H W, Lam M H C, Lau T C and Lo K K W 2009 Novel luminescent tricarbonylrhenium(I) polypyridine tyramine-derived dipicolylamine complexes as sensors for zinc (II) and cadmium (II) ions *Organometallics* **28** 4297
18. Partyka D V, Deligonul N, Washington M P and Gray T G 2009 *fac*-Tricarbonyl rhenium(I) azadipyrromethene complexes *Organometallics* **28** 5837
19. Si Z J, Li X N, Li X Y and Zhang H J 2009 Synthesis, photophysical properties and theoretical studies on pyrrole-containing bromo Re(I) complex *J. Organomet. Chem.* **694** 3742
20. Vogler A and Kunkely H J 2000 Excited state properties of organometallic compounds of rhenium in high and low oxidation states *Coord. Chem. Rev.* **200** 991
21. Lees A J 1998 Organometallic complexes as luminescence process in monitoring thermal and photochemical polymerization *Coord. Chem. Rev.* **177** 3
22. Wang K Z, Huang L, Gao L H, Jin L P and Huang C H 2002 Synthesis, crystal structure and photoelectric properties of Re(CO)$_3$ClL (L= 2-(1-Ethylbenzimidazol-2-yl)pyridine) *Inorg. Chem.* **41** 3353
23. Lundin N J, Blackman A G, Gordon K C and Officer D L 2006 Synthesis and characterization of a multicomponent rhenium(I) complex for application as an OLED Dopant *Angew. Chem., Int. Ed.* **45** 2582
24. Ju C C, Zhang A G, Sun H L, Wang K Z, Jiang W L, Bian Z Q and Huang C H 2011 Synthesis, crystal structure and optical and photoelectrochemical properties of a N∩O⁻ rhenium(I) complex *Organometallics* **30** 712
25. Tsubaki H, Sekine A, Ohashi Y, Koike K, Takeda H and Ishitani O 2005 Control of photochemical, photophysical electrochemical and photocatalytic properties of rhenium(I) complexes using intramolecular weak interactions between ligands *J. Am. Chem. Soc.* **127** 15544
26. Xiong J, Liu W, Wang Y, Cui L, Li Y Z and Zuo J L 2012 Tricarbonyl mono- and dinuclear Rhenium(I) complexes with redox-active bis(pyrazole)-tetrathiafulvalene ligands: Synthesis, crystal structure and properties *Organometallics* **31** 3938
27. Shankar B, Sahu S, Deibel N, Schweinfurth D, Sarkar B, Elumalai P, Gupta D, Hussain F, Krishnamoorthy G and Sathiyendiran M 2014 Luminescent dirhenium(I)-double-heterostranded helicate and mesocate *Inorg. Chem.* **53** 922

28. Wright P J, Muzzioli S, Skelton B W, Raiteri P, Lee J, Koutsantonis G, Silvester D S, Stagni S and Massi M 2013 One-step assembly of Re(I) tricarbonyl 2-pyridyltetrazolato metallacalix [3] arene with aqua emission and reversible three-electron oxidation *Dalton Trans.* **42** 8188

29. Hartmann H, Berger S, Winter R, Fielder J and Kaim W 2000 Reversible and site-specific reduction of the ligand sides in a molecular rectangle with up to eight electrons *Inorg. Chem.* **39** 4977

30. Wu J Y, Chang C H, Thanasekaran P, Tsai C C, Tseng T W, G H Lee, Peng S M and Lu K L 2008 Unusual face-to-face π-π stacking interactions within an indigo-pillared M_3(tpt)-based triangular metalloprism *Dalton Trans.* 6110

31. Bhattacharya D, Chang C H, Cheng Y H, Lai L L, Lu H Y, Lin C Y and Lu K L 2012 Multielectron redox chemistry of a neutral, NIR-active, indigo-pilared Re^I-base triangular metalloprism *Chem. Eur. J.* **18** 5275

32. Nagarajaprakash R, Govindarajan R and Manimaran B 2015 One-pot synthesis of oxamidato-bridged hexarhenium trigonal prisms adorned with ester functionality *Dalton Trans.* **44** 11732

33. Rajakannu P, Shankar B, Yadav A, Shanmugam R, Gupta D, Hussain F, Chang C H, Sathiyendiran M and Lu K L 2011 Adaptation toward restricted conformational dynamics: From the series of neutral molecular rotors *Organometallics* **30** 3168

34. Dinolfo P H, Coropceanu V, Bredas J L and Hupp T 2006 A new class of mixed-valence with orbitally degenerate organic redox centers. Examples based on hexa-rhenium molecular prisms *J. Am. Chem. Soc.* **128** 12592

35. Maji S, Sarkar B, Mobin S M, Fiedler J, Urbanos F A, Aparicio A, Kaim W and Lahiri G K 2008 Intramolecular valency and spin interaction in *meso*- and *rac*- diastereomers of a *p*-quinonoids bridged diruthenium complex *Inorg. Chem.* **47** 5204

36. Haga M, Dodsworth E S and Lever A B P 1986 Catechol-quinone redox series involving bis(pyridine) ruthenium (II) and tetrakis(pyridine) ruthenium (II) *Inorg. Chem.* **25** 447

37. Peover M E and Davies 1963 The influence of ion-association on the polarography of quinines in dimethylformamide *J. Electroanal. Chem.* **6** 46

38. Aljabali A A, Barclay J E, Butt J N, Lomonossoff G P and Evans D J 2010 Redox-active ferocene-modified cowpea mosaic virus nanoparticles *Dalton Trans.* **39** 7569

39. Andrieux C P, Blocman C, Bouchiat J M D, Halla F M and Saveant J M 1980 Homogeneous redox catalysis of electrochemical reactions: Part V cyclic voltammetry *J. Electroanal. Chem.* **113** 19

40. Bhattacharya D, Sathiyendiran M, Lu T T, Chang C H, Cheng Y H, Lin C Y, Lee G H, Peng S M and Lu K L 2009 Ground and excited electronic states of quinone-containing Re(I)-based rectangles: a comprehensive study of their preparation, electrochemistry and photophysics *Inorg. Chem.* **48** 3731

41. Bhattacharya D, Sathiyendiran M, Wu J Y, Chang C H, Huang S C, Zeng Y L, Lin C Y, Thanasekaran P, Lin B C, Hsu C P, Lee G H, Peng S M and Lu K L 2010 Quinonoid-bridged chair-shaped dirhenium(I) metalla-cycles: Synthesis, characterization and spectroelectro-chemical studies *Inorg. Chem.* **49** 10264

42. Gupta D, Shankar B, Elumalai P, Shanmugam R, Mobin S M, Weisser F, Sarkar B and Sathiyendiran M 2014 Synthesis and characterization of a tetrametallic coordination complex of tetrahydroxy-p-benzoquinone *J. Organomet. Chem.* **754** 59

43. Gosztola D, Niemczyk M P and Svec W 2000 Excited double states of electrochemically generated aromatic imide and diimide radical anions *J. Phys. Chem.* **104** 6545

44. Goyal R N and Kumar N 1999 Genetic variants in novel pathways influence blood pressure and cardio-vascular disease risk *Aust. J. Chem.* **52** 43

45. Deibel N, Sommer M G, Hohloch S, Schwann J, Schweinfurth D, Ehertand F and Sarkar B 2014 Dinuclear quinonoid-bridged d^8 metal complexes with redox-active azobenzene stoppers: electrochemical properties and electrochromic behavior *Organometallics* **33** 4756

46. Damas A L, Gullo M P, Rager M N, Jutand A, Barbieri A and Amouri H 2013 Near-infrared room temperature emission from a novel class of Ru(II) heteroleptic complexes with quinonoid organometallic linker *Chem. Commun.* **49** 3796

47. Rajendran T, Manimaran B, Liao R T, Y H Liu, Thanasekaran P, Lin R J, Chang I J, Chou P T, Ramraj R, Rajagopal S and Lu K L 2010 Luminescence quenching of Re(I) molecular rectangles by quinones *Dalton Trans.* **39** 2928